

Development and evaluation of species distribution models for five endangered elasmobranchs in southwestern Atlantic

Sandro Klipper · Silvana Amaral · Lúbia Vinhas

Received: 6 September 2015 / Revised: 12 April 2016 / Accepted: 20 April 2016
© Springer International Publishing Switzerland 2016

Abstract Species distribution models (SDMs) are tools to obtain habitat suitability maps based on historical species occurrences and environmental variables. Those maps can be used to restrict fishing grounds or to assist in planning and reserve selection. This is especially important for species at risk of extinction. We developed SDMs for five endangered elasmobranch species, namely *Squatina guggenheim*, *S. occulta*, *Rhinobatos horkelii*, *Galeorhinus galeus*, and *Mustelus schmitti*, using Boosted Regression Trees. Data from 1,704 bottom trawls carried out between 1972 and 2005 as part of research surveys on the southern Brazilian shelf between 28°36'S and 33°45'S, combined with satellite imagery and environmental atlases, were used in the models. Based on 10-fold cross-validation statistics, all models had a reasonable performance, though *S. guggenheim* models had an excellent discrimination ($AUC > 0.9$) and *R. horkelii* models had just a fair discriminatory power ($AUC 0.7\text{--}0.8$). Except for *R. horkelii*, all models showed good association between observed and predicted occurrences ($PBC > 0.5$). *Squatina guggenheim* models provided the greatest explained deviance

(49–54%), whereas *R. horkelii* models the smallest (14–17%). Models' predictions were consistent with the current knowledge of all species. Moreover, those models made reasonable predictions using the great spatial and temporal coverage of satellite data.

Keywords Chondrichthyes · Species–environment relationships · Essential fish habitat · Threatened species · Boosted regression trees · Remote sensing

Introduction

Species distribution models (SDMs), also known as ecological niche models or realized niche models, relate species occurrence data to environmental variables. These models provide information on the environmental requirements of species and are widely used to predict species distribution, making them important tools for conservation planning and climate change research (Guisan & Zimmermann, 2000; Guisan & Thuiller, 2005; Elith & Leathwick, 2009; Franklin, 2009; Sillero, 2011).

Since 2004, the Brazilian Ministry of Environment has prohibited landing, transport, and sale of five endangered elasmobranch species in Brazil (Vooren & Klipper, 2005). The bottom-dwelling permanent residents *Squatina guggenheim*, *S. occulta*, and *Rhinobatos horkelii* and the free-swimming demersal winter migrants *Galeorhinus galeus* and *Mustelus schmitti*

Handling editor: Begoña Santos

S. Klipper (✉) · S. Amaral · L. Vinhas
Brazilian National Institute for Space Research (INPE),
P.O. Box 515, São José dos Campos, SP 12227-010,
Brazil
e-mail: sandroklipper@gmail.com

were recognized as endangered after a brief period of fisheries exploitation followed by a sudden collapse in their yields (IBAMA, 1995; Vooren, 1997; Miranda & Vooren, 2003). The law has been progressively enforced; however, those species are still caught as bycatch in trawl fisheries. Therefore, we need complementary actions to lower incidental catches of these protected and endangered species, such as no-take areas, where fishing is prohibited (Vooren & Klipper, 2005). Bycatch reduction is one of the biggest challenges for fishery management of elasmobranch species, and the establishment of large protected marine reserves is the most effective strategy for achieving this goal (Musick et al., 2000a, b). In this context, SDMs are useful tools to obtain habitat suitability maps based on historical species occurrences and environmental variables. These maps represent potential habitats where the species may be present or absent (Guisan & Thuiller, 2005; Franklin, 2009; Sillero, 2011). With such knowledge, we could restrict fishing grounds or assist in planning and reserve selection. Moreover, a detailed knowledge of species–environment relationships is essential for understanding many aspects of their ecology. Some relevant examples include the work of Martin et al. (2012), who fitted models for ten elasmobranch species of the eastern English Channel using standard generalized linear model (GLM); Pennino et al. (2013), who employed a Bayesian hierarchical GLM to map sensitive habitats of elasmobranch species in western Mediterranean Sea; and Mendoza et al. (2014), who used classification trees to identify factors that affect the presence of vulnerable elasmobranchs.

Many statistical and machine-learning methods have been introduced to model species' distribution, often with geographic information systems and remote sensing (Guisan & Zimmermann, 2000; Valavanis et al., 2008; Franklin, 2009). Although the generalized additive model (GAM) is perhaps the most common method for modeling fish habitats (Valavanis et al., 2008), several studies have shown that tree-based ensemble models, such as Random Forests (RF) and Boosted Regression Trees (BRT), have superior performance (Elith et al., 2006; Leathwick et al., 2006; Knudby et al., 2010; Bouska et al., 2015). Both are the state-of-the-art among the methods for supervised learning. Although they have similar performance, BRT outperforms RF with simulated data (Hastie et al., 2009).

In this paper, we developed SDMs for *S. guggenheim*, *S. occulta*, *R. horkelii*, *G. galeus*, and *M. schmitti* using BRTs. Data from bottom trawl surveys combined with satellite imagery and environmental atlases were used in the models. The aims of this study were to evaluate the ability of those models to correctly predict the species' occurrence within the surveyed area, and to improve the knowledge of the habitat requirements of these species. In order to aid fishers and stakeholders in operational and resource management decisions to avoid incidental catches, we also assessed the application of remotely sensed data to point out suitable areas for these species.

Materials and methods

Study area

The study area was the southern Brazilian shelf (southwestern Atlantic) between 28°36'S and 33°45'S. It has a surface area of roughly 90,000 km² and an average width of 130 km (Fig. 1a). The bottom sediments are primarily sand in the south of 32°S, whereas mud predominates in the north (Figueiredo Jr. & Madureira, 2004). The area is under the influence of the Subtropical Convergence, confluence between the northward flowing Malvinas (Falkland) Current and the southward flowing Brazil Current, which occurs along the continental slope between 30°S (winter) and 46°S (summer). Hence, environmental conditions have a strong seasonal pattern related to the presence of waters of tropical and subantarctic origin, as well as of the freshwater runoff from La Plata River (~36°S) and Patos Lagoon (~32°S) (Ciotti et al., 1995; Lima et al., 1996; Piola et al., 2000). No consistent, statistically significant pattern of either an increase or a decrease in primary productivity was observed in the study area. In addition, the region had just a moderate increase in sea surface temperature between 1982 and 2006 (Sherman et al., 2009). Therefore, we assumed that the species are at equilibrium with the environment and our data are representative of this condition.

Survey data

The dataset comprises 1,704 bottom trawl hauls of four research vessels carried out between 1972 and

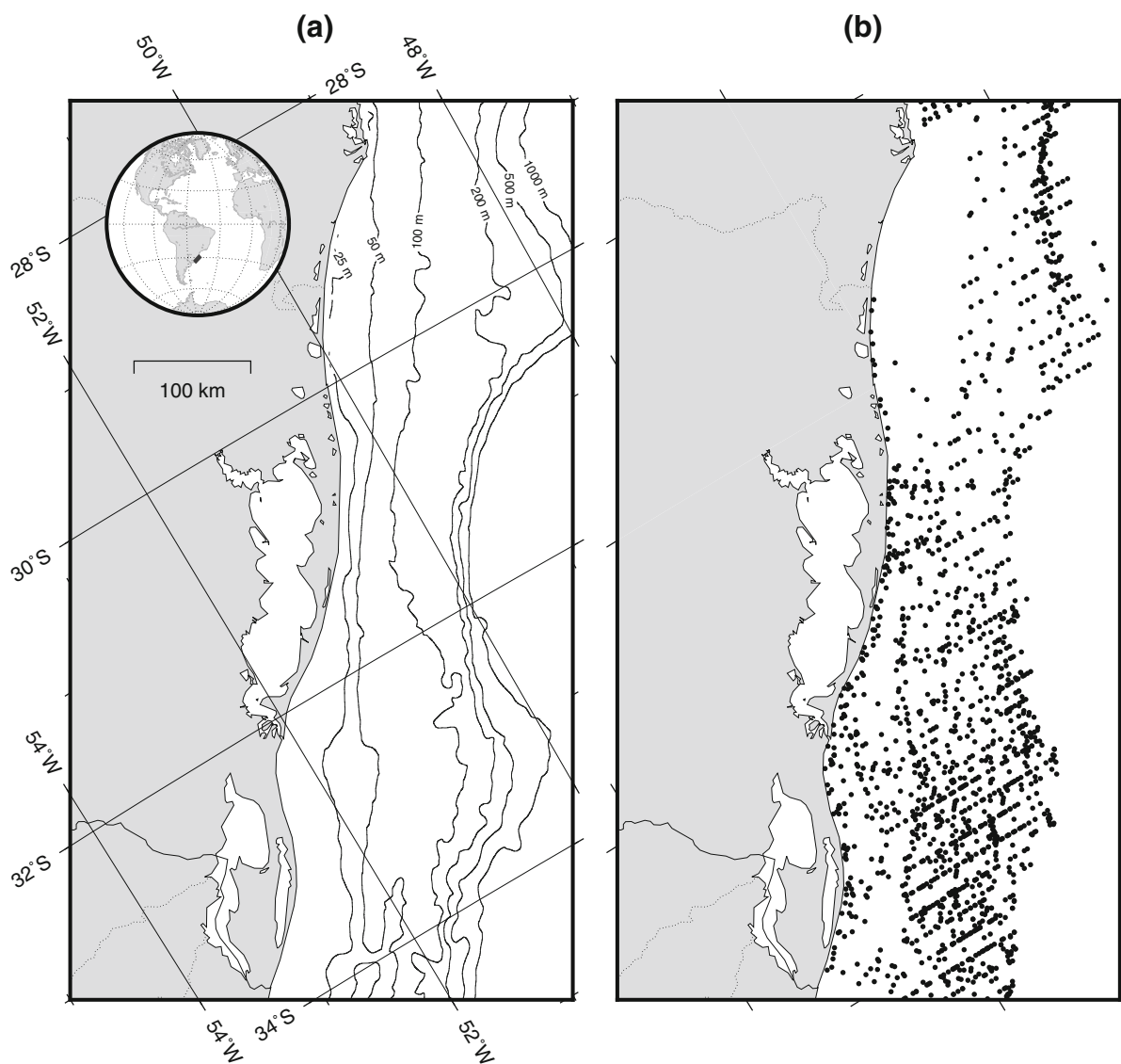


Fig. 1 **a** Map of the study area, showing bathymetric contours and **b** sampling locations ($n = 1,704$). These maps were produced using oblique Mercator projection

2005, from which presence–absence data were drawn (Fig. 1b). Due to limited technical skills of the scientific staff aboard, or because there was not the taxonomic knowledge at the time of sampling, not all species were recorded at each haul. Therefore, absences were only accounted from surveys where the species was registered at least once (Table 1). Trawl duration was usually 30 min, and seven bottom trawl nets were used during the surveys (Table 2). Vooren & Klippel (2005) and Haimovici et al. (2007, 2009) provide descriptions of these vessels and fishing gears.

Environmental predictors

There are three types of environmental predictors: resource, direct, and indirect. Resource predictors are those that are consumed by the species. Direct predictors are environmental parameters that have physiological importance, but are not consumed. Indirect predictors are those that have no direct physiological relevance, but they are easily measured in the field and have good correlation with observed species pattern, often replacing a combination of different resources and direct variables (Guisan &

Table 1 Endangered elasmobranchs in southwestern Atlantic for which species distribution models were developed

Scientific name	Common name	Presences/absences	Prevalence
<i>Galeorhinus galeus</i> (Linnaeus, 1758)	Tope Shark	512/758	0.40
<i>Mustelus schmitti</i> Springer, 1939	Smooth-hound Shark	866/560	0.61
<i>Squatina occulta</i> Vooren & Silva, 1991	Hidden Angel Shark	178/311	0.36
<i>Squatina guggenheim</i> Marini, 1936	Angular Angel Shark	284/192	0.60
<i>Rhinobatos horkelii</i> Müller & Henle, 1841	Brazilian Guitarfish	217/360	0.38

It is also shown the number of presences and absences, as well as their prevalence

Table 2 Summary of bottom trawl nets used to catch the species modeled

Cod	Trawl net	Period	Source
G1	49.3-m-footrope-length high-opening fish trawl	1982–1983	Haimovici et al. (2007)
G2	52.9-m-footrope-length low-opening fish trawl	1980–1981	Haimovici et al. (2007)
G3	28-m-footrope-length high-opening fish trawl	1972–1978	Haimovici et al. (2007)
G4	25.5-m-footrope-length semi-balloon shrimp trawl	1973	Haimovici et al. (2007)
G5	20-m-footrope-length shrimp trawl	2005	Vooren & Klipper (2005)
G6	28-m-footrope-length fish trawl w/steel bobbins	1986–1987	Haimovici et al. (2007)
G7	40.4-m rockhopper Engel Star balloon trawl	2001–2002	Haimovici et al. (2009)

Zimmermann, 2000). We chose eight environmental predictors (Table 3) that had some postulated connection to the ecological requirements of the species (Menni & Stehmann, 2000; Vögler et al., 2008; Cortés et al., 2011; Martin et al., 2012; Pennino et al., 2013) and for which pairwise Pearson correlations between variables were less than 0.6.

Depth and bottom water temperature are the main environmental gradients along which the elasmobranchs are distributed in southwestern Atlantic (Menni et al., 2010). Temperature and salinity are environmental parameters that have physiological importance, and have direct influence on elasmobranch distribution at all spatial scales (Simpfendorfer & Heupel, 2004), whereas depth is an indirect proxy for several functionally relevant predictors, such as temperature, salinity, light, and pressure (Elith & Leathwick, 2009). Chlorophyll concentration gives a broad indication of primary productivity, and as such the surface temperature can be used to detect the position of thermal fronts and marine productivity hotspots (Valavanis et al., 2008). The spatial gradient of surface temperature points out the place where a front between water masses occurs. Moreover,

previous studies on elasmobranchs have shown that the seabed type and slope are important predictors of species distribution (Martin et al., 2012; Pennino et al., 2013). The predictors were drawn from three sources by selecting the first available, in this order: (1) in situ data, (2) satellite imagery, and (3) environmental atlases. Hence, in the absence of in situ data, we take records from satellite imagery, and in the lack of satellite imagery, we pick up mean values from climatological fields. Measured concurrently with species' observations, in situ data include surface and bottom temperatures, bottom salinity, and average depth of each haul. The average depth was always registered. Surface and bottom temperatures were measured in 90% and 83% of the surveyed sites, whereas bottom salinity was recorded in only 18% of the sites.

Satellite imagery came from AVHRR and SeaWiFS sensors. AVHRR-derived daily surface temperatures were taken from NOAA V2 High-resolution Blended Analysis of Daily SST according to Reynolds et al. (2007). Data are available from September 1, 1981 on a $\frac{1}{4}$ -degree resolution grid. From these data, we built daily grids of spatial gradient of surface

Table 3 Environmental predictors used in the models

Predictor	Mean (range)	Availability	Source
Depth	119 m (7–587)	All sites	In situ
Slope	0.54° (0–7.4)	All sites	ETOPO1-derived
Surface temperature	18.8°C (10–26.8)	90% of the sites	In situ
	19.9°C (12.1–25.0)	Daily values from Sep 1, 1981 onwards	AVHRR-derived
	19.3°C (11.6–25.8)	Monthly climatology	WOA 2013
Bottom temperature	15.9°C (4–25.4)	83% of the sites	In situ
	16.6°C (3–24.1)	Monthly climatology	WOA 2013
Bottom salinity	33.5 psu (22–36.7)	18% of the sites	In situ
	35.2 psu (31–36.7)	Monthly climatology	WOA 2013
Chlorophyll concentration	1.28 mg m ⁻³ (0.1–5.4)	Monthly values from September 1997 to December 2010	
	1.45 mg m ⁻³ (0.1–6.5)	Monthly climatology	SeaWiFS-derived
Spatial gradient of surface temperature	0.06°C km ⁻¹ (0–0.25)	Daily values from September 1, 1981 onwards	
	0.07°C km ⁻¹ (0–0.21)	Monthly climatology	AVHRR-derived
Seabed sediment type	—	All sites	Digitized map

temperature (sstgrad) by calculating the centered differencing. Further, we take the average values over the period from 1981 to 2014 to make monthly climatological fields. SeaWiFS-derived chlorophyll was obtained from NASA Goddard Space Flight Center, Ocean Ecology Laboratory, Ocean Biology Processing Group (2014). Monthly chlorophyll concentrations are available from Sep, 1997 to Dec, 2010, as well as monthly climatology, on a 9-km resolution grid.

From environmental atlases, we drew temperature and salinity values from the World Ocean Atlas 2013. It includes monthly climatological fields for temperature and salinity at standard depth levels with a spatial resolution of $\frac{1}{4}$ -degree (Locarnini et al., 2013; Zweng et al., 2013). In addition, sea floor slope was derived from ETOPO1 Global Relief Model at 1/60-degree resolution (Amante & Eakins, 2009) using GRASS GIS (Neteler & Mitasova, 2008). Finally, seabed sediment type was extracted from a digitized map. The scale of the original paper map was 1/1,100,000 and it was published by Figueiredo Jr. & Madureira (2004). Based on the proportions of sand, mud, and gravel, they classified the bottom sediments into ten classes, namely sand, mud, gravel, sandy mud,

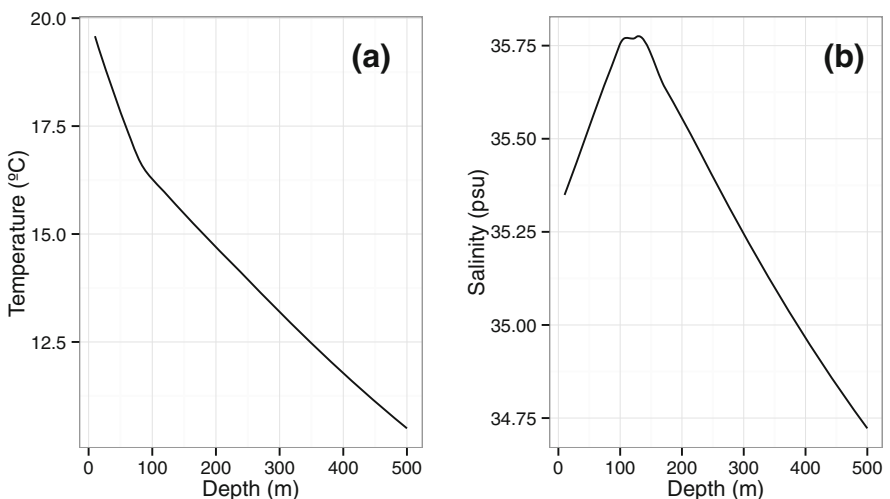
sandy gravel, muddy sand, muddy gravel, gravelly sand, gravelly mud, and sand/mud/gravel.

In the relationship between species occurrence and bottom temperature, depth is invariably a confounding variable and should be taken into account. Therefore, instead of using directly bottom temperature as a predictor, we used the difference between the bottom temperature and the expected temperature at a given depth (temperature residual). The expected temperature was given by local polynomial regression (Hastie et al., 2009) fitted on bottom temperature estimates at each site (Fig. 2a). Hence, if the resultant temperature residual (tempresid) is negative, the water is colder than the average. Otherwise, if it is positive, the water is warmer than the average. Similarly, we fitted a regression relating salinity to depth (Fig. 2b), and we extracted the residuals from this (salresid). This approach resembles that adopted by Leathwick et al. (2006).

Model development and evaluation

All models were fitted and evaluated in R (R Core Team, 2015) using the gbm library (Ridgeway, 2015) and code provided by Elith et al. (2008) plus custom

Fig. 2 Average relationships between **a** depth and temperature and **b** depth and salinity, as predicted by local polynomial regression fitted on all data



code. Using presence–absence data as a response variable, we modeled the species' joint probability of occurrence and capture as a function of environmental predictors through logistic regressions. To fit the logistic regressions, we used boosted regression trees (BRT) with binomial deviance loss function. There are three hyper-parameters in BRT models: number of trees, learning rate, and tree complexity. Tree complexity (also known as interaction depth) was set to five, allowing up to five-variable interaction effects. A higher value seldom provides significant improvement (Hastie et al., 2009). The optimal number of trees increases as the learning rate is decreased. Hence, the learning rate was chosen among the values 0.01, 0.005, or 0.001, to ensure at least 1,000 trees as suggested by Elith et al. (2008). The optimal number of trees was identified through deviance reduction using 10-fold cross-validation (Hastie et al., 2009), and then a final model was fitted using all data.

BRT learns the relationship between the response and its predictors rather than assume a data model and estimate its parameters. To do this, it uses two algorithms in a stagewise procedure. The boosting algorithm successively adds a new decision tree after re-weighting the residuals. The decision-tree algorithm, in turn, recursively splits the predictor space, choosing at each step the best predictor and cutpoint that minimizes the weighted residuals. The final model is an ensemble that combines many decision trees (Elith et al., 2008; Hastie et al., 2009). In this way, BRT models overcome most issues described by Zuur et al. (2010) that can lead to wrong statistical models.

They do not suffer from the inclusion of irrelevant predictors and outliers, handle different types of predictor and response variables, and can automatically fit interaction effects between predictors (Elith et al., 2008). In addition, unlike linear models and generalized linear models, a BRT model does not have multicollinearity issues, since it largely ignores redundant predictors. However, there is no *P* value for rejection of null hypothesis and it is not easy to determine the degrees of freedom (Elith et al., 2008). Therefore, instead of examining the statistical validity, we adopted a pragmatic approach to model building and variable selection that emphasizes models' ability to predict well. Beginning with a broad set of relevant predictors, alternate models were constructed by removing the less influential variable and by selecting those that are easier to measure in terms of effort and cost.

For each species, three competing models were built by selecting subsets of the environmental predictors: (1) 'full', the complete set of environmental predictors; (2) 'base,' without sediment type (seabed), which was the less influential predictor; and (3) 'pruned,' with just depth, slope, surface temperature, and chlorophyll. In addition, null models with no predictors, against which all others were compared, were estimated using the mean probability of occurrence across the study area (prevalence).

Different fishing gears vary in efficiency in catching individual species. Therefore, to account for catch efficiency of the distinct types of trawl nets employed, we followed the pragmatic approach used by

Leathwick et al. (2008), where the fishing method was added into the models as a categorical variable. Here, we added a categorical covariate (geartype) with seven classes, where each class represents a trawl net described in Table 2. Besides, we assume that the different research vessels behaved similarly.

We employed a 10-fold cross-validation to estimate the predictive ability of those models with new data (Pearce & Ferrier, 2000; Hastie et al., 2009). The average values and standard errors of residual deviance, area under ROC curve (AUC), and point biserial correlation coefficient (PBC) were computed from the subsets of data excluded from the model fitting. In addition, the proportion of explained deviance (D^2), which is the proportion by which a model reduces null deviance, was calculated. AUC, PBC, and D^2 are threshold-independent measures; therefore, probabilities did not need to be transformed into binary outcome using a specific cut-off value before evaluation. AUC and PBC provide the discriminatory power of the models, whereas D^2 reports the reliability of the models (Liu et al., 2011).

The receiver operating characteristic (ROC) curve was used for assessing the tradeoff between true-positive and false-positive rates, of which the AUC is a quantitative summary. AUC was estimated using the Mann–Whitney U statistic. It ranges from 0.5 for models with no discrimination ability to 1.0 for models with perfect discrimination. The values between 0.5 and 0.7 indicate poor discrimination capacity because true-positive rate is not much more than false-positive rate (Pearce & Ferrier, 2000). PBC was calculated as the Pearson correlation coefficient between the observed presence–absence (dichotomous variable) and the predicted probability (Liu et al., 2011). D^2 is equivalent to R^2 in linear regression models, and it is a helpful statistic to evaluate competing models. It ranges from 0.0 for the null model to 1.0 for perfect models with no residual deviance (Guisan & Zimmermann, 2000; Hosmer & Lemeshow, 2000; Franklin, 2009).

The contribution of each environmental predictor to the models was evaluated using a function implemented in the gbm library. It is calculated as the relative influence of each predictor in reducing the loss function. Additional details about computations can be found in Hastie et al. (2009). We used partial dependence plots to evaluate the marginal effect of each environmental predictor of the models base and

pruned on probability of occurrence. To do this, the geartype covariate was fixed at the first trawl net (G1), and all other predictors were held constant at their mean values. These partial dependence plots show the effect of each predictor on probability of occurrence after accounting for the average effects of the other predictors (Hastie et al., 2009).

Finally, we used average probabilities of capture to assess the relative efficiency of the fishing gears employed. They were estimated for each geartype class as the joint probability of occurrence and capture given by the base model, holding all environmental predictors at their mean values.

Model mapping

Partial dependence plots are helpful to interpret the effects of environmental predictors on probability of occurrence; however, they are limited to low-dimensional views, which prevent us from assessing high-order interactions, and may include value combinations of environmental predictors that actually do not occur in geographic space. Therefore, rather than building complex graphic representations, we made monthly probability maps of species occurrence as predicted by the base models using climatological data and standardized to a common trawl net (G1). Then, to assess the ecological validity of the relationships fitted, we compared those maps with species' distribution and behavior reported in the literature. The monthly climatological data came from World Ocean Atlas 2013 (temperature and salinity), SeaWiFS (chlorophyll), and AVHRR (spatial gradient of surface temperature). We also used ETOPO1-derived depth and slope. The finer grids were resampled to the same spatial resolution of the World Ocean Atlas 2013 (1/4-degree) by averaging.

Additionally, we used pruned models to make spatial predictions from satellite imagery instead of using climatological data. We employed two Aqua MODIS 8-day composites (August 13–20, 2014 and December 19–26, 2014) of sea surface temperature (11 μ nighttime) and chlorophyll concentration downloaded from the NASA Ocean Color Web data portal (<http://oceancolor.gsfc.nasa.gov>). Depth and slope from ETOPO1 were resampled to match the 4-km resolution of MODIS.

We used a bootstrapping procedure for uncertainty quantification. We drew 1,000 samples with re-

placement of the input data and made predictions. Once they were accumulated, we calculated the 5th–95th percentile range for each grid cell and took half of this value as an estimate of the error associated with models' outcomes.

Results

Measures of discrimination capacity and reliability of the models are presented in Table 4. Based on 10-fold cross-validation statistics, all models had a reasonable performance ($AUC > 0.7$) though *Squatina guggenheim* models had an excellent discrimination ($AUC > 0.9$) and *Rhinobatos horkelii* models had just a fair discriminatory power ($AUC 0.7$ – 0.8). The point biserial correlation coefficient (PBC) ranged from 0.40 to 0.79 and it was minimal in *R. horkelii* models and maximal in *S. guggenheim* models. Except for *R. horkelii*, all models showed good association between observed and predicted occurrences ($PBC > 0.5$).

Cross-validated proportion of explained deviance (D^2) ranged from 14% to 54%. The species models that provided the greatest explained deviance were *S. guggenheim* with 49–54%, whereas the smallest explained deviance was provided in the *R. horkelii* models with 14–17%. Comparison of performance statistics for the three model types (full, base, and pruned) indicated that the full model did not explain more deviance than the base model for *Galeorhinus galeus*, *Mustelus schmitti*, and *Squatina occulta*. In addition, for *R. horkelii* and *S. guggenheim*, full model had a slightly greater predictive power, explaining one and two percent more deviance than the base model, respectively. All pruned models had a slightly lesser predictive power than the base models, explaining one to three percent less deviance. However, the discriminatory power did not significantly reduce, holding a reasonable performance (Table 4).

Seabed type was the lowest relevant contributor in the full models of all species (Table 5). Its contribution ranged from 0.7% to 4.4% and was highest in *S. occulta*.

Table 4 Predictive performance of BRT models and the number of covariates and trees fitted

	Model	No. of covariates	No. of trees	CV residual deviance (SE)	D^2	CV AUC (SE)	CV PBC (SE)
<i>G. galeus</i>	Full	9	1050	0.940 (0.022)	0.30	0.85 (0.008)	0.61 (0.011)
	Base	8	2,000	0.939 (0.039)	0.30	0.85 (0.013)	0.61 (0.026)
	Pruned	5	1,350	0.960 (0.032)	0.29	0.84 (0.012)	0.59 (0.022)
	Null	0	–	1.349	0.00	0.50	–
<i>M. schmitti</i>	Full	9	1,550	1.004 (0.029)	0.25	0.81 (0.013)	0.56 (0.020)
	Base	8	1,400	0.986 (0.019)	0.26	0.82 (0.009)	0.58 (0.014)
	Pruned	5	1,550	0.993 (0.022)	0.26	0.82 (0.010)	0.57 (0.017)
	Null	0	–	1.340	0.00	0.50	–
<i>S. occulta</i>	Full	9	4,050	0.984 (0.039)	0.25	0.83 (0.017)	0.55 (0.029)
	Base	8	4,450	0.977 (0.044)	0.25	0.84 (0.018)	0.55 (0.034)
	Pruned	5	3,550	0.994 (0.036)	0.24	0.81 (0.015)	0.53 (0.029)
	Null	0	–	1.311	0.00	0.50	–
<i>S. guggenheim</i>	Full	9	5,350	0.625 (0.049)	0.54	0.93 (0.009)	0.79 (0.021)
	Base	8	4,100	0.648 (0.050)	0.52	0.92 (0.013)	0.78 (0.024)
	Pruned	5	3,000	0.694 (0.052)	0.49	0.90 (0.018)	0.77 (0.027)
	Null	0	–	1.349	0.00	0.50	–
<i>R. horkelii</i>	Full	9	2,850	1.105 (0.029)	0.17	0.77 (0.017)	0.44 (0.029)
	Base	8	2,800	1.106 (0.042)	0.16	0.77 (0.023)	0.44 (0.045)
	Pruned	5	2,400	1.139 (0.017)	0.14	0.74 (0.013)	0.40 (0.021)
	Null	0	–	1.324	0.00	0.50	–

The average values of residual deviance, area under ROC curve (AUC), and point biserial correlation coefficient (PBC), as well as their standard error (SE) values, were calculated using 10-fold cross-validation (CV). D^2 is the proportion by which a model reduces null deviance

guggenheim. Leaving it out of the base model only did few adjustments in the weight of the other predictor variables. As a result, the discriminatory power was not significantly reduced. In fact, it even grew in *M. schmitti* (Table 4). Slope had the highest influence in *S. guggenheim* models, whereas depth had its highest influence in *S. occulta* models. Surface temperature and chlorophyll concentration were the major predictors for *G. galeus* and *M. schmitti*, whereas tempresid and salresid had their highest weight in the models of *S. guggenheim*, *S. occulta*, and *R. horkelii* (Table 5).

Overall, all species were most commonly caught using trawl nets for fish than shrimp trawls. Similarly, trawl nets equipped with steel bobbins or rubber disks for use on rough seabed had lower success than those without them. The catch of *G. galeus* was apparently favored by trawl nets with higher vertical opening. In contrast, for *S. occulta*, *S. guggenheim*, and *R. horkelii*, a trawl net with low vertical opening had slightly greater success (Table 6).

The partial dependence plots of the marginal effect on probability of occurrence exhibited nonlinear relationships with explanatory variables and differed subtly between base and pruned models (Fig. 3). The marginal effect had no clear relationship with surface temperature, except in *G. galeus* models that had maximum positive influence around 12.5–15.0°C. On the other hand, in almost all models, marginal effect on probability of occurrence showed direct or inverse relationship with chlorophyll concentration. In *M. schmitti*, *S. guggenheim*, and *R. horkelii* models, the marginal effect increased from about 0.5 mg m⁻³ to

Table 6 Average probabilities of capture of the fishing gears employed, given by the base models

	G1	G2	G3	G4	G5	G6	G7
<i>G. galeus</i>	0.36	0.34	0.36	—	—	0.32	—
<i>M. schmitti</i>	0.69	0.69	0.67	0.35	0.23	0.24	—
<i>S. occulta</i>	0.31	0.43	—	—	—	0.39	0.14
<i>S. guggenheim</i>	0.85	0.86	—	—	0.10	0.21	0.21
<i>R. horkelii</i>	0.35	0.37	—	—	0.27	—	0.32

about 4.0 mg m⁻³ of chlorophyll, whereas it decreased in *S. occulta* models in the same range. The *G. galeus* models had their highest values of marginal effect with chlorophyll concentration of around 2.0 mg m⁻³. The marginal effect on probability of occurrence slightly increased from 0.0 to 0.2°C km⁻¹ of surface temperature gradient in *S. occulta* model and exhibited an opposite trend in *R. horkelii* model. *Galeorhinus galeus* and *M. schmitti* models had also an approximate inverse relationship between 0.05 and 0.15°C km⁻¹ and *S. guggenheim* model had no clear pattern with surface temperature gradient (Fig. 3).

Partial dependence plots indicated that *G. galeus* occurred at depths below 50 m, mainly around 100 and 300 m deep on continental slopes (slope ≥ 3) and in colder and less saline waters. They also indicated that *M. schmitti* occurred at depths up to 300 m though it was more frequent at around 50 m depth on continental shelves (slope < 1). Both *S. occulta* and *S. guggenheim* occurred more often in warmer waters.

Table 5 Contribution of each environmental predictor to the BRT models

	<i>G. galeus</i>			<i>M. schmitti</i>			<i>S. occulta</i>			<i>S. guggenheim</i>			<i>R. horkelii</i>		
	Full	Base	Pruned	Full	Base	Pruned	Full	Base	Pruned	Full	Base	Pruned	Full	Base	Pruned
Depth	19	19.6	24.5	9.7	9.5	12.6	42.8	41.9	58	14.1	16.4	24.5	26.6	27.1	37.9
Slope	7.1	6.8	9.7	7.9	8.2	12.4	8.8	9.1	16.2	16.6	17.6	31.2	14.4	13.8	22.3
Surface temperature	41.5	42.4	52.9	32.6	35.1	44.9	7.1	7.5	10.3	10.3	9.6	15.9	5.9	6.1	10.8
Chlorophyll	9.6	9.3	12.8	23	23.1	30.2	9	8.8	15.4	18.7	20.8	28.4	18.9	19	29.1
Sstgrad	7.5	7.7	—	8.2	7.9	—	6.7	7.1	—	6.3	5.8	—	6.5	6.5	—
Tempresid	7.4	7.8	—	11.1	11.2	—	11	11.4	—	13.1	12.8	—	18.3	18.7	—
Salresid	6	6.3	—	5.7	5	—	13.9	14.2	—	16.5	16.9	—	8.3	8.7	—
Seabed	1.8	—	—	1.8	—	—	0.7	—	—	4.4	—	—	1.1	—	—

Relative influence of each predictor is scaled so that the sum adds to 100

However, *S. guggenheim* was mainly found up to 100 m depth on continental shelves and *S. occulta* was found at the depths of 50–300 m, mainly on continental slopes. In addition, *S. occulta* was less tolerant with waters of low salinity than *S. guggenheim*. *Rhinobatos horkelii* occurred in warm and low-salinity waters on continental shelves up to 150 m deep, but mainly at depths around 50 m (Fig. 3).

Together with spatially distributed habitat information, those species–environment relationships were taken back to geographic space as maps of monthly probability of occurrence as predicted by the base models (Figs. 4, 5, 6, 7, 8). As a result, those maps showed that *G. galeus* was absent from October to May and it occurred mainly on the outer shelf (>50 m) in southern area (Fig. 4). *Mustelus schmitti* was more widely distributed than *G. galeus*, occurring in all months on the continental shelf, though it also showed a seasonal displacement pattern (Fig. 5). *Squatina guggenheim* was also widely distributed on the continental shelf; however, it exhibited only a subtle displacement over the summer months (Fig. 6). *Squatina occulta* occurred in all months, but mainly on the outer shelf (Fig. 7). The maps of *R. horkelii* had the lowest probabilities of occurrence over the study area. Nevertheless, they showed distinct spatial patterns. Overall, in spring and summer months the highest probability values were close to the southern coast, whereas in the autumn and winter they were spread over the continental shelf (Fig. 8).

In addition, probability of occurrence for each species was mapped by pruned models using satellite imagery data for two distinct weeks in 2014. The pattern was similar to those provided by base models but with finer resolution (Fig. 9). As a result, *G. galeus* was predicted to be common in the southernmost continental shelf below 50 m deep in August. Moreover, high probabilities of occurrence were predicted in some spots on the outer shelf (Fig. 9a). In contrast, it was predicted to be absent in December (Fig. 9b). High probabilities of occurrence were predicted across the continental shelf for *M. schmitti* in August (Fig. 9c). While it was also present in December, the highest probabilities of occurrence were predicted at around 50 m depth in southern area (Fig. 9d). *Squatina occulta* was spread over the outer shelf in August. High probabilities of occurrence were predicted only in some spots of the northern area (Fig. 9e). On the other hand, it was clustered along

the isobath of 100 m in December (Fig. 9f). *Squatina guggenheim* was predicted to be common over the continental shelf both in August (Fig. 9g) and in December (Fig. 9h) with subtle differences. The highest probabilities of occurrence for *R. horkelii* in August were predicted between the southern latitudes of 30 and 32°, up to 50 m deep (Fig. 9i). In December, this area was extended to 34° of southern latitude (Fig. 9j). Prediction errors associated with models' predictions tended to be higher in areas where individuals were caught more frequently. Conversely, errors were lower in areas where individuals were caught less frequently (Fig. 10). This indicated that there was little model uncertainty concerning the extent of the areas where the modeled species was absent.

Discussion

In this paper, data from bottom trawl surveys were used to model the joint probability of occurrence and capture of elasmobranchs as a function of environmental variables. Although fishing gear differences are not considered a drawback with presence–absence data (Menni et al., 2010), here we used the geartype covariate to account for catch efficiency of the different types of trawl nets employed. We acknowledge that our approach is rather pragmatic and perhaps the use of descriptors for every trawl parameter would be better, but it was not feasible here given the lack of detailed data about each tow. Nevertheless, the results were as expected, showing the highest probabilities of capture in trawl nets for fish (Table 6). However, those values must be interpreted with care because different gears were employed at distinct epochs. As they actually represent the joint probability of occurrence and capture and not only the trawl efficiency, values in Table 6 might include temporal effects such as overexploitation.

In order to account for yearly changes in probability of occurrence due to overexploitation, we could add a variable describing the year in the models, allowing only a monotonic decrease on its marginal effect. This constraint can be easily specified in a BRT model (Leathwick et al., 2006; Ridgeway, 2015). Even so, it is not possible to disentangle the temporal effects from catch efficiency. As a solution, we did not attempt to examine those effects separately. Instead, we used the

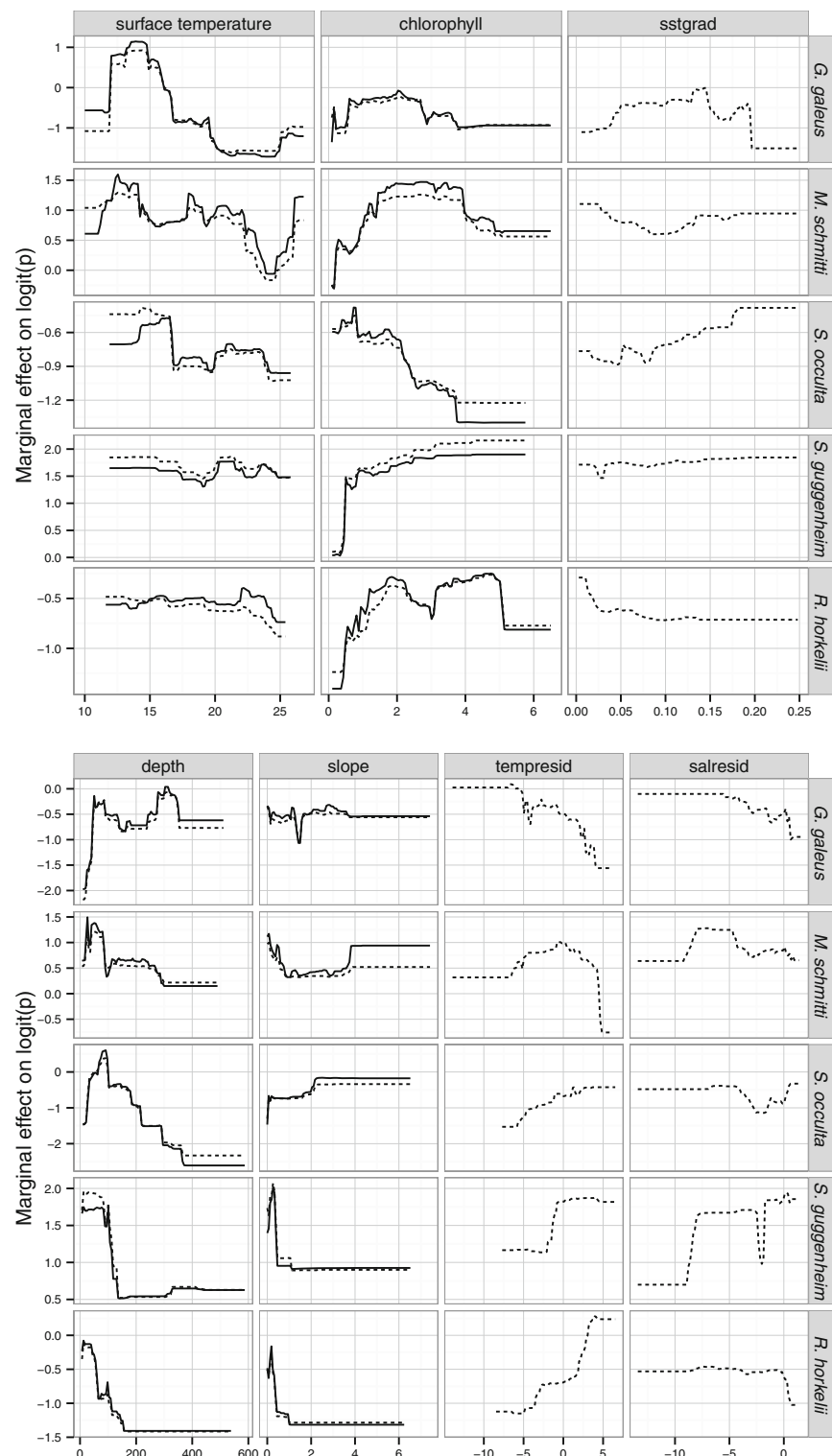


Fig. 3 Partial dependence on probability of occurrence in the models: base (dashed line) and pruned (solid line)

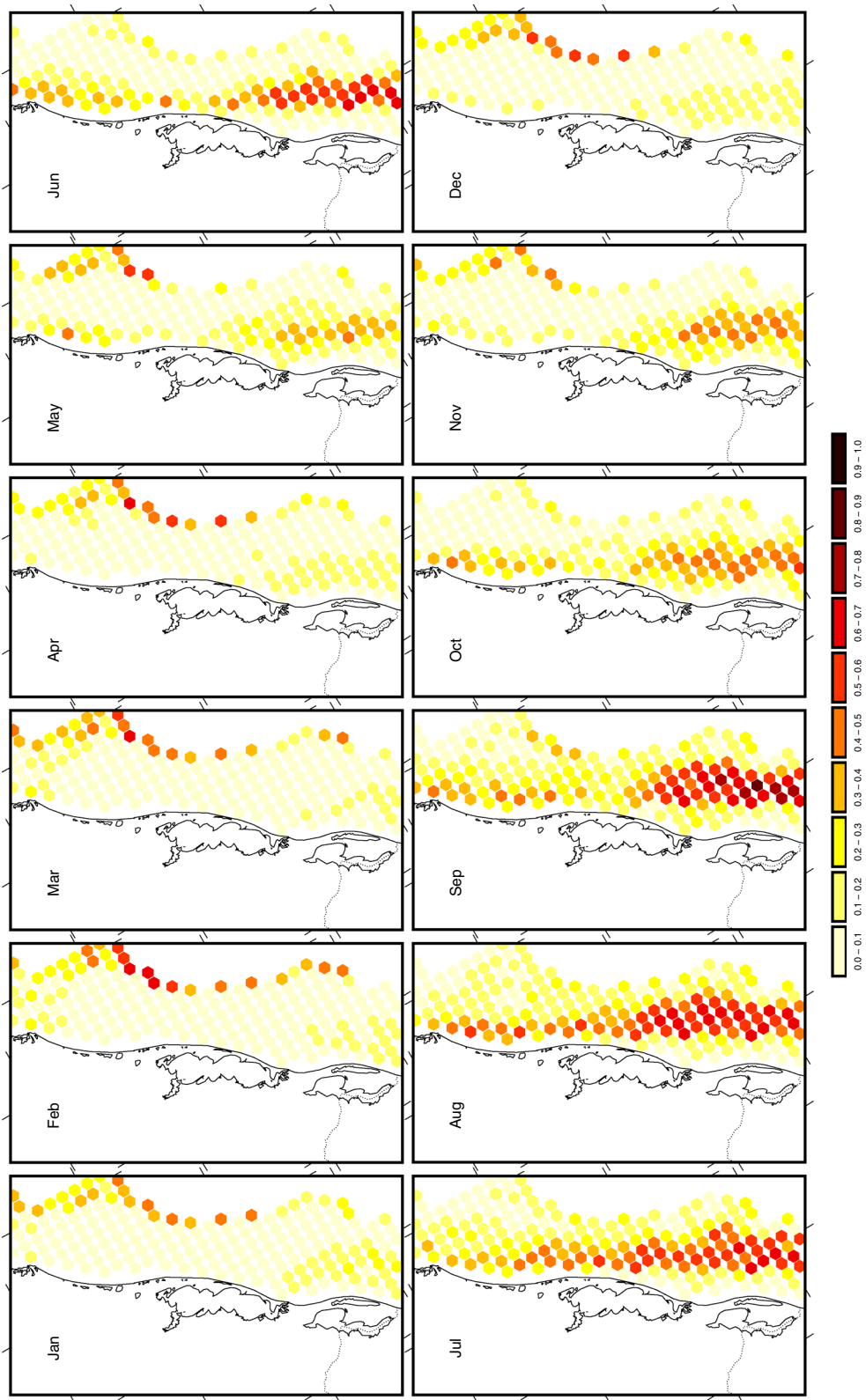


Fig. 4 Monthly maps of the presence probability for *G. galeus* per standardized trawl obtained from the base model

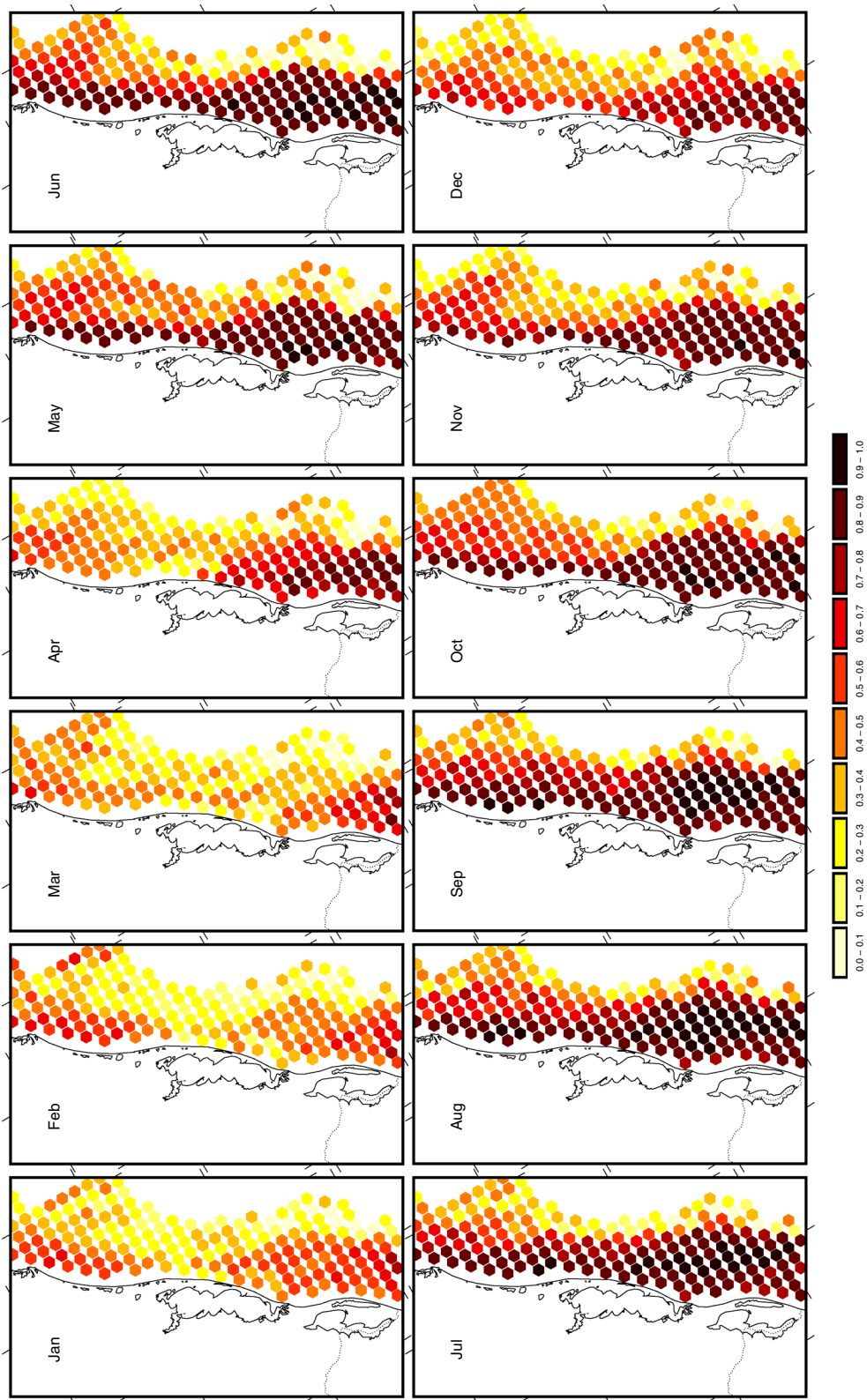


Fig. 5 Monthly maps of the presence probability for *M. schmitti* per standardized trawl obtained from the base model

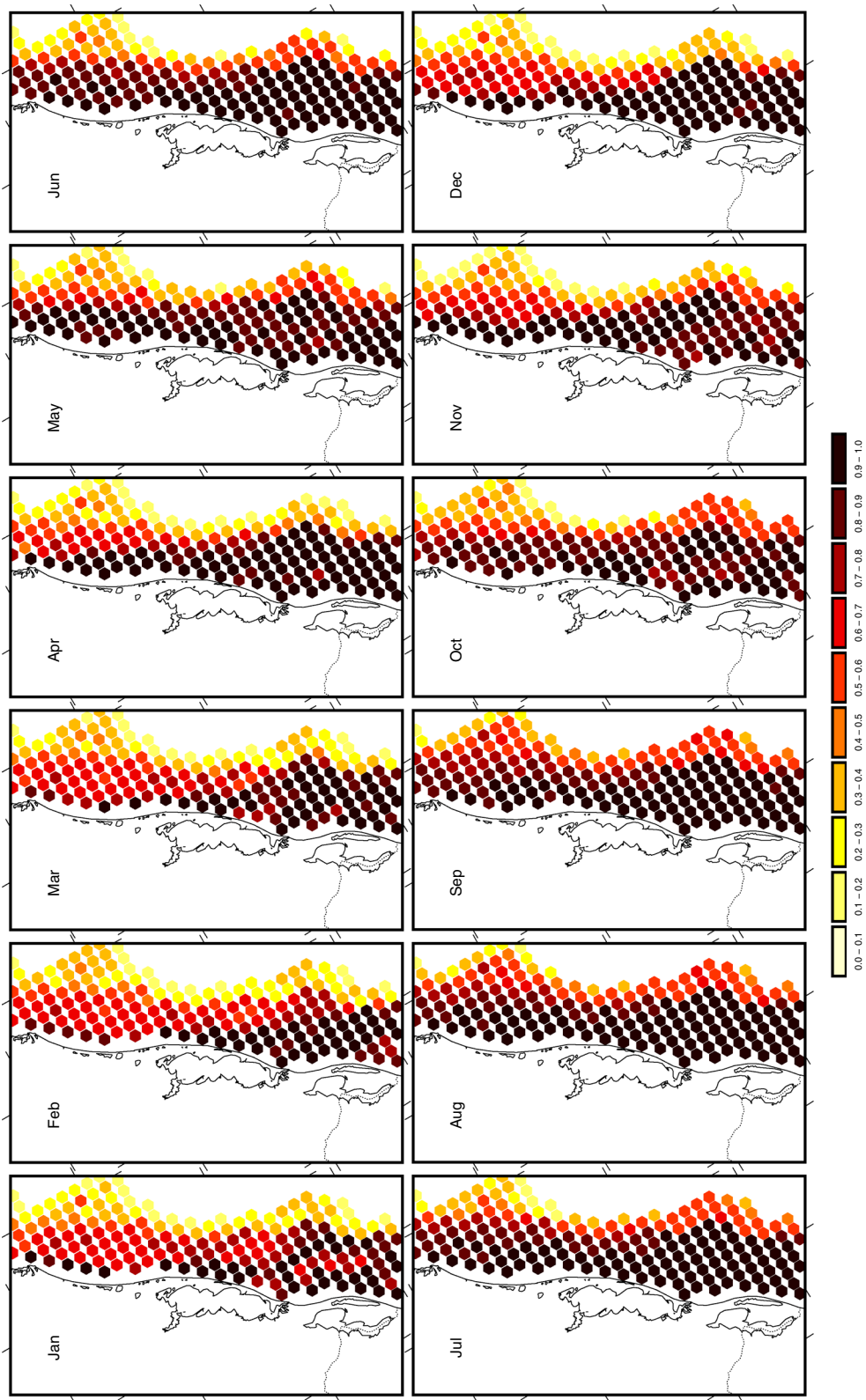


Fig. 6 Monthly maps of the presence probability for *S. guggenheim* per standardized trawl obtained from the base model

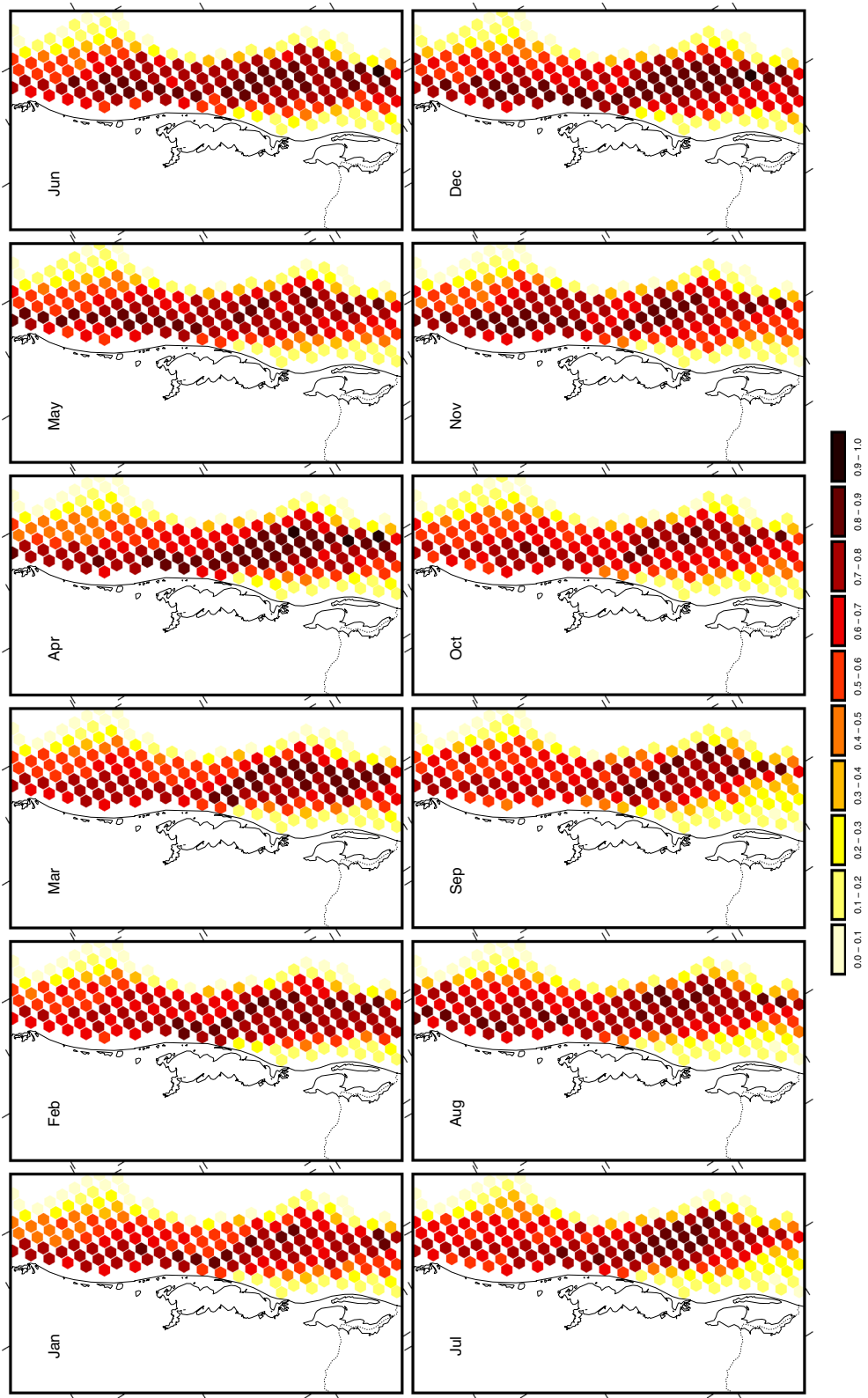


Fig. 7 Monthly maps of the presence probability for *S. occultus* per standardized trawl obtained from the base model

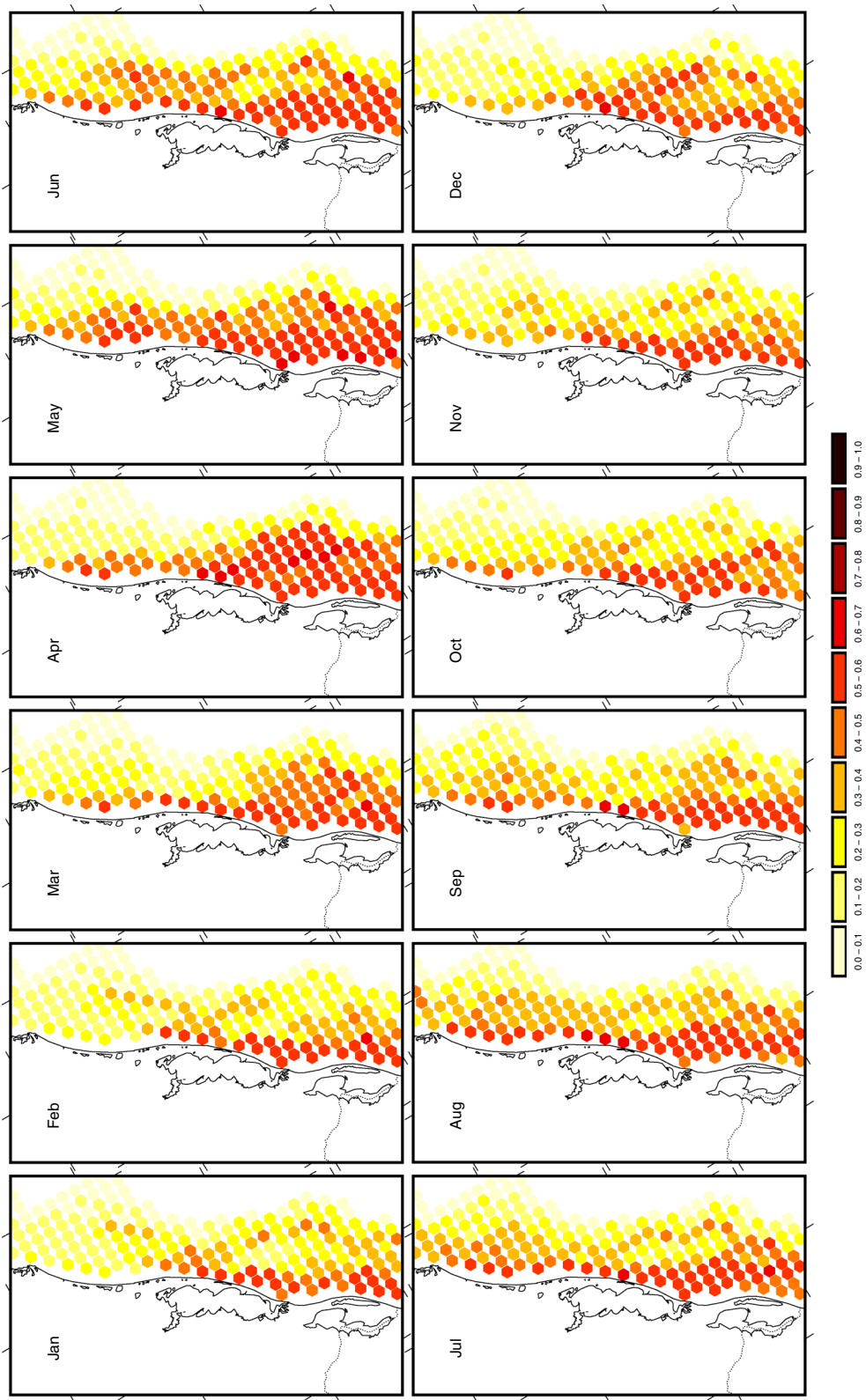


Fig. 8 Monthly maps of the presence probability for *R. horkelii* per standardized trawl obtained from the base model

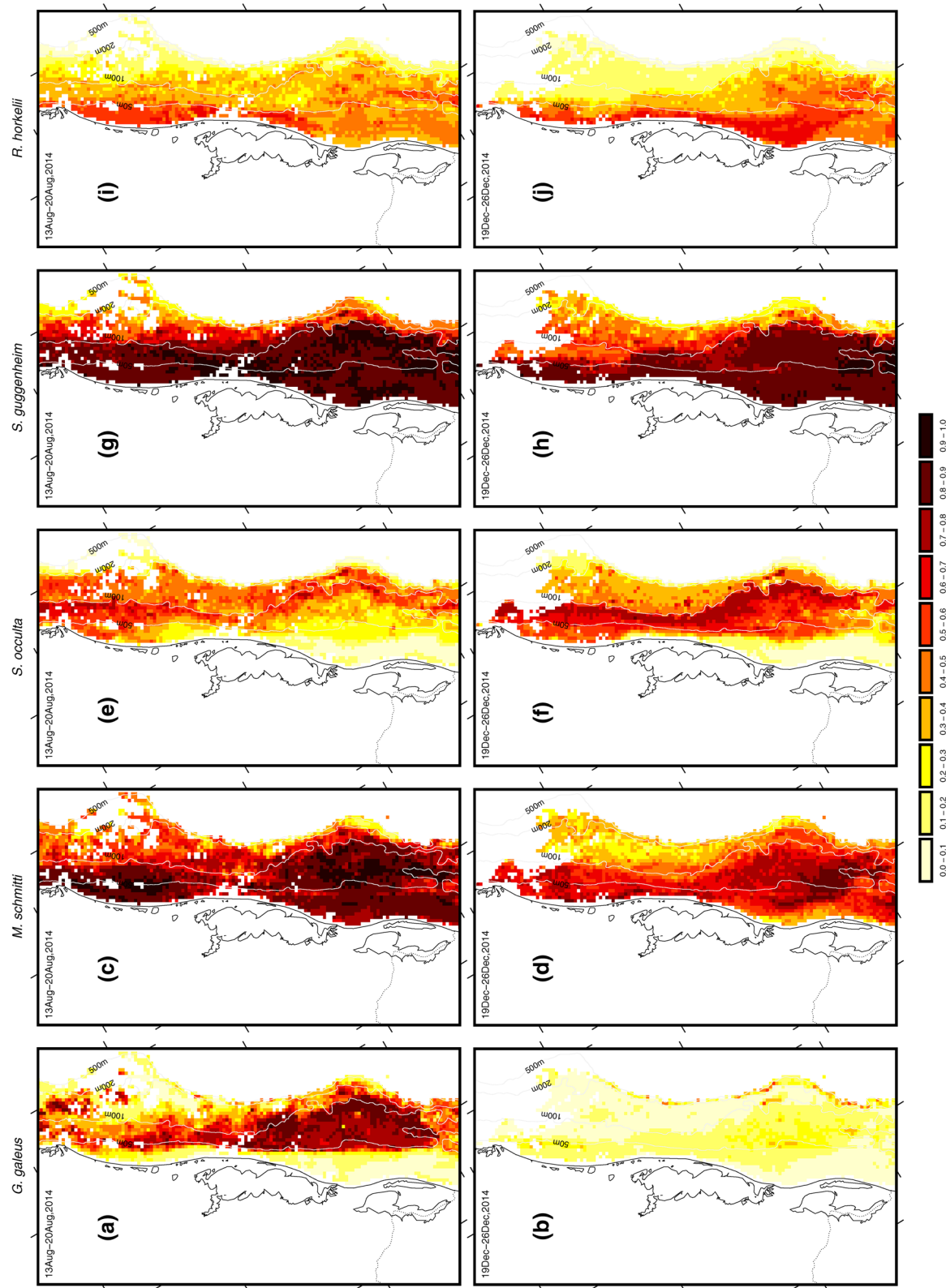


Fig. 9 Probability of occurrence as predicted by the pruned model using satellite imagery for two distinct weeks: 13 August–20 August 2014 and 19 December–26 December 2014

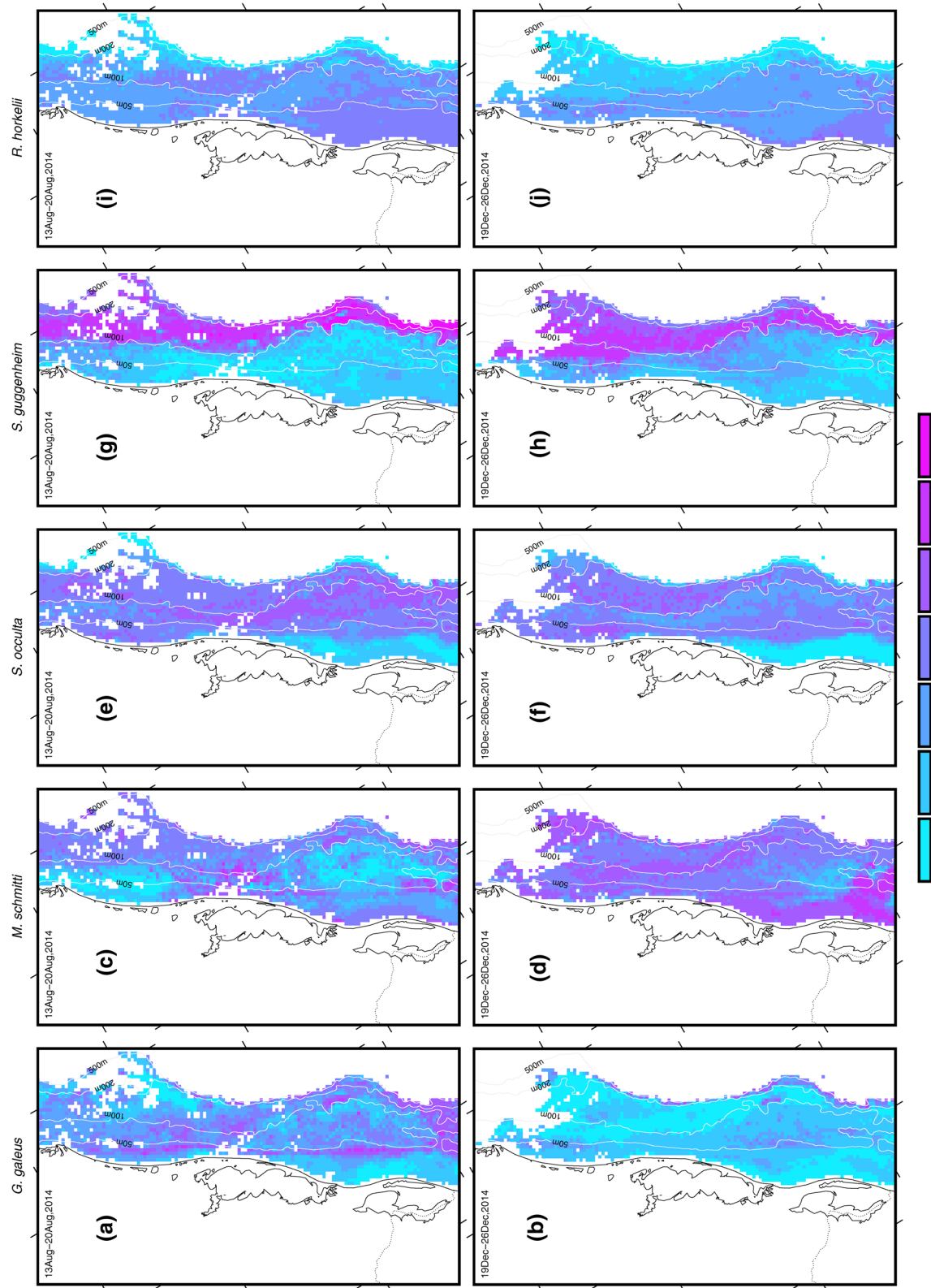


Fig. 10 Prediction error associated with the pruned model, estimated by bootstrapping species, boosted regression trees, and remote sensing

geartype covariate just to tune the model. In this way, it handles both temporal and gear effects, and thus it should not be used for inference. Although simple, this approach allowed us to make use of all data available so far to focus on major environmental determinants of species distributions.

Unlike findings reported for elasmobranch species in the western Mediterranean Sea (Pennino et al., 2013) and in the eastern English Channel (Martin et al., 2012), the low relative influence of seabed type suggests that it is not an important determinant of species' distribution in the area and at the spatial scale of this work. Although our sampling was limited to trawlable sites, and probably did not include hard-bottom surfaces, bottom sediments on southern Brazilian shelf are mainly composed of sand and mud (Figueiredo Jr. & Madureira, 2004). Therefore, we do not expect a significant bias in that result.

Our results showed that depth was a strong predictor of occurrence of all species. Indeed, Vooren (1997) has already noted that those species inhabit distinct depth ranges in the study area. This also agrees with studies that modeled elasmobranch distributions in other regions, whose depth was the main predictor (Martin et al., 2012; Pennino et al., 2013). In contrast, Vögler et al. (2008) stated that depth had no influence on *Squatina guggenheim* distribution in southwestern Atlantic off Argentina. We must note, however, that over the depth where the species occurs (<100 m) there is no remarkable change in the marginal effect on probability of occurrence with depth (Fig. 3). Therefore, within this depth range, the probability of occurrence of this species is almost constant indeed. Notwithstanding, elasmobranch species composition has high correlation with depth in the southwestern Atlantic (Menni et al., 2010). Together with depth, slope is a surrogate for describing continental margin habitats and had a high influence on probability of occurrence of all species (Table 5).

Surface temperature and chlorophyll concentration had higher influence on distribution of free-swimming sharks *Galeorhinus galeus* and *Mustelus schmitti* than in the other species (Table 5). *Galeorhinus galeus* prefers surface temperatures below 17°C, whereas *M. schmitti* occurs over a wider range of temperatures, but with no clear pattern (Fig. 3). This is consistent with the observed temperatures of occurrence of *G. galeus* (8.0–16.5°C) and *M. schmitti* (7.6–21.6°C) in the southwestern Atlantic using an independent dataset

(Menni et al., 2010). Although *G. galeus* is more responsive to temperature change than *M. schmitti*, both seem to follow the seasonal displacement of waters of subantarctic origin in the region. In winter, cold low-salinity waters from the Argentinian shelf occupy most of the study area, while by late spring these waters begin to retreat to the south (Lima et al., 1996), which is when *G. galeus* leaves the area (Fig. 4). *Mustelus schmitti*, in turn, is widely distributed in the study area, except in the summer (Fig. 5), when warmer and salty waters of tropical origin predominate over the continental shelf (Lima et al., 1996). Indeed, there is consensus that both species migrate to breed in Argentinian and Uruguayan waters during late spring and summer (Peres & Vooren, 1991; Lucifora et al., 2004; Oddone et al., 2005; Cortés et al., 2011). *Mustelus schmitti* has an annual reproductive cycle (Oddone et al., 2005), while *G. galeus* has a triennial cycle (Peres & Vooren, 1991; Lucifora et al., 2004). A triennial reproductive cycle means that only a portion of the population has to take part in reproductive movements. Therefore, it is likely that these migrations are also associated with the use of the subsurface front between subtropical and subantarctic shelf waters as feeding grounds (Acha et al., 2004; Lucifora et al., 2012).

Analyses of bottom temperature residuals suggest that the bottom-dwelling elasmobranchs *Squatina guggenheim*, *S. occulta*, and *Rhinobatos horkelii* occur in warmer waters than *G. galeus* and *M. schmitti* (Fig. 3). In geographic terms, they are predicted to occur throughout the year in the study area (Figs. 6, 7, 8). *Squatina guggenheim* and *R. horkelii* are associated with waters of high chlorophyll concentrations ($>2.0 \text{ mg m}^{-3}$), whereas *S. occulta* occurs mainly in waters of low chlorophyll concentrations. In addition, the probability of occurrence of *S. occulta* rises in sharp temperature gradients (Fig. 3). Higher chlorophyll concentrations are related to the coastal water, a mixture of shelf waters, and freshwater outflow that occupies the inner shelf. In contrast, low chlorophyll concentrations are located in offshore areas, mainly under the influence of tropical waters (Ciotti et al., 1995). As a result, *S. guggenheim* and *R. horkelii* are predicted to occur mainly on inner shelf, whereas *S. occulta* is predicted to occur on outer shelf and shelf break (Figs. 6, 7, 8).

Squatina guggenheim, *S. occulta*, and *R. horkelii* complete their life cycles within the region, but

pregnant females and neonates of *S. occulta* are rarely found (Vooren, 1997). Females of *S. guggenheim* have a three-year reproductive cycle, with parturition taking place in spring and summer at shallow waters (Vooren & Klipper, 2005; Colonello et al., 2007). As just part of the population migrates seasonally and we did not analyze the data by sex and reproductive stage, our maps do not show seasonal bathymetric displacements. However, there is a subtle southward displacement in summer months (Fig. 6). This pattern is consistent with that observed in coastal waters off northern Argentina and Uruguay (34–38°S) where the abundance of *S. guggenheim* was higher in spring than in winter (Colonello et al., 2007).

Vögler et al. (2008) have suggested that the coastal waters off northern Argentina and Uruguay under the influence of the freshwater discharge from the La Plata River are birth and nursery areas of *S. guggenheim*. In waters off southern Brazil, neonates of *S. guggenheim* were found only south of 32°S (Vooren & Klipper, 2005), which is in turn the northern boundary of the low-salinity plume of the La Plata River in summer (Piola et al., 2000). We believe that this low-salinity plume bounds a large nursery area of *S. guggenheim*, encompassing shallow waters off southern Brazil, Uruguay, and northern Argentina. The high biological production of those waters can provide food and shelter for neonates and first-year juveniles (Acha et al., 2004). Therefore, pregnant females of *S. guggenheim* migrate to this area to give birth during spring and summer. This raises the species' probability of occurrence, which is captured by our model through the environmental variables. Although the low-salinity plume reaches 28°S in winter, it retracts to 32°S in summer (Piola et al., 2000), which explains the lower predicted probability of occurrence in the north of the study area during the summer months (Fig. 6). According to our hypothesis, there must be some exchange between the *S. guggenheim* populations in southwestern Atlantic.

Both *R. horkelii* and *S. guggenheim* were observed in most landings from trawling and gillnets at Itajai harbor (27°S), whose fleets worked in the whole southern Brazil (Mazzoleni & Schwingel, 1999). However, unlike *S. guggenheim*, the base model for *R. horkelii* predicted low probabilities of occurrence throughout the study area (Fig. 8). The low explained deviance (14–17%) indicates that the *R. horkelii* models have little predictive power. In contrast, for

example, the proportion of explained deviance reaches 54% for *S. guggenheim*. Although the explained deviance is a metric particularly useful to evaluate competing models (Hosmer & Lemeshow, 2000; Franklin, 2009), the low percentage of explained deviance might indicate that we are missing important environmental determinants of the distribution of *R. horkelii*. Another explanation is that there are also key biotic factors underlying the distribution of this species. As stated by Simpfendorfer & Heupel (2004), the needs to feed, avoid predators, and reproduce should drive the habitat selection by elasmobranchs too. For instance, the reproductive cycle of *R. horkelii* is annual and synchronous. The gestation takes 12 months, but the embryonic development occurs only in the last 4 months. Females increase embryonic development rate through migration to a warmer environment after a period of dormancy of the fertilized eggs (Lessa et al., 1986; Vooren & Klipper, 2005). To account for this trait, it would need to investigate sex-specific environmental relationships as suggested by Vögler et al. (2008). Regardless of low percentage of explained deviance, our models for *R. horkelii* had reasonable discriminatory power as indicated by AUC values higher than 0.7. This means a probability higher than 70% to correctly distinguish between occupied and unoccupied sites (Pearce & Ferrier, 2000).

All competing models had a discriminatory power significantly better than by chance alone. Moreover, their reliabilities were equivalent, since the explained deviance only changed from one to three percent between the models. However, leaving out the seabed type variable resulted in a more parsimonious model. Further, although pruned models had the fewest variables, they did not lose predictive power. In this case, surface temperature and chlorophyll might act as surrogates for bottom temperature and salinity. Indeed, the amount of chlorophyll is directly related to the water masses present in the study area (Ciotti et al., 1995). In this way, ocean surface measurements from satellite remote sensing can also be used to reveal sub-surface conditions (Santos, 2000). This is an important finding because satellite imagery provides synoptic ocean measurements. We need to measure these variations to correctly predict marine fish distributions since ocean features may change over the seasons and inter-annually (Valavanis et al., 2008; Klemas, 2013).

Consequently, our models can be used to make reasonable predictions using the great spatial and temporal coverage of satellite data. Such performance is particularly useful to restrict fishing grounds, or even to prompt fishers to move to areas with lesser probability of incidental catches (Stuart et al., 2011). Moreover, by focusing management measures on key areas and important habitats, we move toward an ecosystem approach to fisheries management (Valavanis et al., 2008). Besides assisting in conservation planning and population management, they can also be used to predict species distributions under climate change (Hijmans & Graham, 2006; Elith & Leathwick, 2009; Hollowed et al., 2013).

Conclusion

We provide a better understanding of the environmental factors influencing the distribution of five endangered elasmobranch species in southwestern Atlantic. More significantly, though, unlike previous studies that have focused on univariate analyses or qualitative inferences on environmental relationships, our models allow prediction of a species' distribution in order to assist rational marine resource management. The predicted distributions are also baseline information for which future changes in species distributions, management practices, and the effects of climate change may be monitored and compared. This is especially important for species at risk of extinction. To our knowledge, this study is also the first to use SDM in southwestern Atlantic. It is noteworthy that the models' predictions were consistent with the current knowledge about those species. Nevertheless, further studies are necessary to investigate ontogenetic and sex-specific environmental relationships of those species.

References

- Acha, E. M., H. W. Mianzan, R. A. Guerrero, M. Favero & J. Bava, 2004. Marine fronts at the continental shelves of austral South America. *Journal of Marine Systems* 44: 83–105.
- Amante, C. & B. W. Eakins, 2009.ETOPO1 1 Arc-Minute Global Relief Model: Procedures, Data Sources and Analysis. National Geophysical Data Center, NOAA, <http://www.ngdc.noaa.gov/mgg/global/global.html>.
- Bouska, K. L., G. W. Whittlestone & C. Lant, 2015. Development and evaluation of species distribution models for fourteen native central U.S. fish species. *Hydrobiologia* 747: 159–176.
- Ciotti, Á. M., C. Odebrecht, G. Fillmann & O. O. Moller, 1995. Freshwater outflow and subtropical convergence influence on phytoplankton biomass on the southern Brazilian continental shelf. *Continental Shelf Research* 15: 1737–1756.
- Colonello, J. H., L. O. Lucifora & A. M. Massa, 2007. Reproduction of the angular angel shark (*Squatina guggenheim*): geographic differences, reproductive cycle, and sexual dimorphism. *ICES Journal of Marine Science* 64: 131–140.
- Cortés, F., A. J. Jaureguizar, R. C. Menni & R. A. Guerrero, 2011. Ontogenetic habitat preferences of the narrownose smooth-hound shark, *Mustelus schmitti*, in two Southwestern Atlantic coastal areas. *Hydrobiologia* 661: 445–456.
- Elith, J. & J. R. Leathwick, 2009. Species distribution models: ecological explanation and prediction across space and time. *Annual Review of Ecology Evolution and Systematics* 40: 677–697.
- Elith, J., C. H. Graham & NCEAS Modeling Group, 2006. Novel methods improve prediction of species' distributions from occurrence data. *Ecography* 29: 129–151.
- Elith, J., J. R. Leathwick & T. Hastie, 2008. A working guide to boosted regression trees. *Journal of Animal Ecology* 77: 802–813.
- Figueiredo Jr, A. G. & L. S. P. Madureira, 2004. Topografia, composição, refletividade do substrato marinho e identificação de províncias sedimentares na Região Sudeste-Sul do Brasil. Instituto Oceanográfico, São Paulo.
- Franklin, J., 2009. Mapping Species Distributions: Spatial Inference and Prediction. Cambridge University Press, Cambridge.
- Guisan, A. & W. Thuiller, 2005. Predicting species distribution: offering more than simple habitat models. *Ecology Letters* 8: 993–1009.
- Guisan, A. & N. E. Zimmermann, 2000. Predictive habitat distribution models in ecology. *Ecological Modelling* 135: 147–186.
- Haimovici, M., A. Olinto, L. V. de M. Miranda & S. Klippel, 2007. Prospecções na região sudeste-sul. In Haimovici, M. (ed.), A prospecção pesqueira e abundância de estoques marinhos no Brasil nas décadas de 1960 a 1990: Levantamento de dados e avaliação crítica. MMA/SMCQ, Brasília: 35–73.
- Haimovici, M., L. Gomes Fischer, C. L. D. B. S. R. Rossi-Wongtschowski, R. Avila Bernardes & R. Aguiar dos Santos, 2009. Biomass and fishing potential yield of demersal resources from the outer shelf and upper slope of southern Brazil. *Latin American Journal of Aquatic Research* 37: 395–408.
- Hastie, T., R. Tibshirani & J. H. Friedman, 2009. The Elements of Statistical Learning: Data Mining, Inference, and Prediction. Springer, New York, NY.
- Hijmans, R. J. & C. H. Graham, 2006. The ability of climate envelope models to predict the effect of climate change on species distributions. *Global Change Biology* 12: 2272–2281.
- Hollowed, A. B., E. N. Curchitser, C. A. Stock & C. I. Zhang, 2013. Trade-offs associated with different modeling

- approaches for assessment of fish and shellfish responses to climate change. *Climatic Change* 119: 111–129.
- Hosmer, D. W. & S. Lemeshow, 2000. *Applied Logistic Regression*. Wiley, New York.
- IBAMA, 1995. Peixes demersais. IBAMA/MMA, Brasília.
- Klemas, V., 2013. Fisheries applications of remote sensing: an overview. *Fisheries Research* 148: 124–136.
- Knudby, A., A. Brenning & E. LeDrew, 2010. New approaches to modelling fish-habitat relationships. *Ecological Modelling* 221: 503–511.
- Leathwick, J., J. Elith, M. Francis, T. Hastie & P. Taylor, 2006. Variation in demersal fish species richness in the oceans surrounding New Zealand: an analysis using boosted regression trees. *Marine Ecology Progress Series* 321: 267–281.
- Leathwick, J. R., J. Elith, W. L. Chadderton, D. Rowe & T. Hastie, 2008. Dispersal, disturbance and the contrasting biogeographies of New Zealand's diadromous and non-diadromous fish species. *Journal of Biogeography* 35: 1481–1497.
- Lessa, R. P., C. M. Vooren & J. Lahaye, 1986. Desenvolvimento e ciclo sexual das fêmeas, migrações e fecundidade da viola *Rhinobatos horkelii* (Mueller & Henle, 1841) do Sul do Brasil. *Atlântica* 8: 5–34.
- Lima, I. D., C. A. E. Garcia & O. O. Möller, 1996. Ocean surface processes on the southern Brazilian shelf: characterization and seasonal variability. *Continental Shelf Research* 16: 1307–1317.
- Liu, C., M. White & G. Newell, 2011. Measuring and comparing the accuracy of species distribution models with presence-absence data. *Ecography* 34: 232–243.
- Locarnini, R. A., A. V. Mishonov, J. I. Antonov, T. P. Boyer, H. E. Garcia, O. K. Baranova, M. M. Zweng, C. R. Paver, J. R. Reagan, D. R. Johnson, M. Hamilton & D. Seidov, 2013. World Ocean Atlas 2013, Vol. 1: Temperature. NOAA: 40 pp. <http://www.nodc.noaa.gov/OC5/woa13/>.
- Lucifora, L. O., R. C. Menni & A. H. Escalante, 2004. Reproductive biology of the school shark, *Galeorhinus galeus*, off Argentina: support for a single southwestern Atlantic population with synchronized migratory movements. *Environmental Biology of Fishes* 71: 199–209.
- Lucifora, L. O., V. B. García, R. C. Menni & B. Worm, 2012. Spatial patterns in the diversity of sharks, rays, and chimaeras (Chondrichthyes) in the Southwest Atlantic. *Biodiversity and Conservation* 21: 407–419.
- Martin, C. S., S. Vaz, J. R. Ellis, V. Lauria, F. Coppin & A. Carpentier, 2012. Modelled distributions of ten demersal elasmobranchs of the eastern English Channel in relation to the environment. *Journal of Experimental Marine Biology and Ecology* 418–419: 91–103.
- Mazzoleni, R. C. & P. R. Schwingel, 1999. Elasmobranch species landed in Itajaí harbor, southern Brazil. *Notas Técnicas Facimar* 3: 111–118.
- Mendoza, M., D. Garrido & J. M. Bellido, 2014. Factors affecting the fishing impact on cartilaginous fishes in southeastern Spain (western Mediterranean Sea). *Scientia Marina* 78: 67–76.
- Menni, R. C. & M. F. W. Stehmann, 2000. Distribution, environment and biology of batoid fishes off Argentina, Uruguay and Brazil, a review. *Revista del Museo Argentino de Ciencias Naturales* 2: 69–109.
- Menni, R. C., A. J. Jaureguizar, M. F. W. Stehmann & L. O. Lucifora, 2010. Marine biodiversity at the community level: zoogeography of sharks, skates, rays and chimaeras in the southwestern Atlantic. *Biodiversity and Conservation* 19: 775–796.
- Miranda, L. V. & C. M. Vooren, 2003. Captura e esforço de pesca de elasmobrânquios demersais no sul do Brasil nos anos de 1975 a 1997. *Frente Marítimo* 19: 217–231.
- Musick, J. A., S. A. Berkeley, G. M. Cailliet, M. Camhi, G. Huntsman, M. Nammack & M. L. Warren, 2000a. Protection of Marine Fish Stocks at Risk of Extinction. *Fisheries* 25: 6–8.
- Musick, J. A., G. Burgess, G. Cailliet, M. Camhi & S. Fordham, 2000b. Management of Sharks and Their Relatives (Elasmobranchii). *Fisheries* 25: 9–13.
- NASA Goddard Space Flight Center, Ocean Ecology Laboratory, Ocean Biology Processing Group, 2014. SeaWiFS Ocean Color Data. NASA Goddard Space Flight Center, Ocean Ecology Laboratory, Ocean Biology Processing Group. 10.5067/ORBVIEW-2/SEAWIFS_OC.2014.0.
- Neteler, M. & H. Mitasova, 2008. *Open Source GIS: A GRASS GIS Approach*. Springer, New York.
- Oddone, M. C., L. Paesch & W. Norbis, 2005. Reproductive biology and seasonal distribution of *Mustelus schmitti* (Elasmobranchii: Triakidae) in the Rio de la Plata oceanic front, south-western Atlantic. *Journal of the Marine Biological Association UK* 85: 1193–1198.
- Pearce, J. & S. Ferrier, 2000. Evaluating the predictive performance of habitat models developed using logistic regression. *Ecological Modelling* 133: 225–245.
- Pennino, M. G., F. Muñoz, D. Conesa, A. López-Quílez & J. M. Bellido, 2013. Modeling sensitive elasmobranch habitats. *Journal of Sea Research* 83: 209–218.
- Peres, M. B. & C. M. Vooren, 1991. Sexual development, reproductive cycle, and fecundity of the school shark *Galeorhinus galeus* off southern Brazil. *Fishery Bulletin* 89: 655–667.
- Piola, A. R., E. J. D. Campos, O. O. Möller, M. Charo & C. Martinez, 2000. Subtropical shelf front off eastern South America. *Journal of Geophysical Research* 105: 6565.
- R Core Team, 2015. R: A Language and Environment for Statistical Computing. R Foundation for Statistical Computing, Vienna. <http://www.R-project.org/>.
- Reynolds, R. W., T. M. Smith, C. Liu, D. B. Chelton, K. S. Casey & M. G. Schlax, 2007. Daily high-resolution-blended analyses for sea surface temperature. *Journal of Climate* 20: 5473–5496.
- Ridgeway, G., 2015. gbm: Generalized Boosted Regression Models. R Package Version 2.1.1. <http://CRAN.R-project.org/package=gbm>.
- Santos, A. M. P., 2000. Fisheries oceanography using satellite and airborne remote sensing methods: a review. *Fisheries Research* 49: 1–20.
- Sherman, K., I. M. Belkin, K. D. Friedland, J. O'Reilly & K. Hyde, 2009. Accelerated warming and emergent trends in fisheries biomass yields of the world's large marine ecosystems. *AMBIO: A Journal of the Human Environment* 38: 215–224.
- Sillero, N., 2011. What does ecological modelling model? A proposed classification of ecological niche models based

- on their underlying methods. *Ecological Modelling* 222: 1343–1346.
- Simpfendorfer, C. A. & M. R. Heupel, 2004. Assessing habitat use and movement. In Carrier, J., J. Musick & M. Heithaus (eds), *Biology of Sharks and Their Relatives*. CRC Press, Boca Raton, FL: 553–572.
- Stuart, V., T. Platt & S. Sathyendranath, 2011. The future of fisheries science in management: a remote-sensing perspective. *ICES Journal of Marine Science* 68: 644–650.
- Valavanis, V. D., G. J. Pierce, A. F. Zuur, A. Palialaxis, A. Saveliev, I. Katara & J. Wang, 2008. Modelling of essential fish habitat based on remote sensing, spatial analysis and GIS. *Hydrobiologia* 612: 5–20.
- Vögler, R., A. C. Milesi & R. A. Quiñones, 2008. Influence of environmental variables on the distribution of *Squatina guggenheim* (Chondrichthyes, Squatinidae) in the Argentine-Uruguayan Common Fishing Zone. *Fisheries Research* 91: 212–221.
- Vooren, C. M., 1997. Demersal elasmobranchs. In Seeliger, U., C. Odebrecht & J. P. Castello (eds), *Subtropical Convergence Environments: The Coast and Sea in the Southwestern Atlantic*. Springer, Berlin: 141–146.
- Vooren, C. M. & S. Klippel (eds), 2005. *Ações para a conservação de tubarões e raias no sul do Brasil*. Igaré, Porto Alegre.
- Zuur, A. F., E. N. Ieno & C. S. Elphick, 2010. A protocol for data exploration to avoid common statistical problems: data exploration. *Methods in Ecology and Evolution* 1: 3–14.
- Zweng, M. M., J. R. Reagan, J. I. Antonov, R. A. Locarnini, A. V. Mishonov, T. P. Boyer, H. E. Garcia, O. K. Baranova, D. R. Johnson, D. Seidov & M. M. Biddle, 2013. World Ocean Atlas 2013, Vol. 2: Salinity. NOAA: 39 pp. <http://www.nodc.noaa.gov/OC5/woa13/>.